

# UNCLASSIFIED

<b>AD NUMBER</b>
AD000242
<b>NEW LIMITATION CHANGE</b>
<b>TO</b> Approved for public release, distribution unlimited
<b>FROM</b> No Foreign distribution
<b>AUTHORITY</b>
USAMERDL ltr., 20 Jun 1972

THIS PAGE IS UNCLASSIFIED

Reproduced by

**Armed Services Technical Information Agency**  
**DOCUMENT SERVICE CENTER**

**KNOTT BUILDING, DAYTON, 2, OHIO**

**AD -**

**242**

**UNCLASSIFIED**

AD No. 242  
ASTIA FILE COPY

Report No. 6

on

Contract DA-44-009-ng 406  
Project 8-74-01-00

F. N. Cassette  
September 17, 1955

**THE OHIO STATE UNIVERSITY  
RESEARCH FOUNDATION**

# REPORT

By

THE OHIO STATE UNIVERSITY  
RESEARCH FOUNDATION  
COLUMBUS 10, OHIO

Cooperator ..... ENGINEER RESEARCH AND DEVELOPMENT  
LABORATORIES, Fort Belvoir, Virginia  
..... Contract DA-44-009eng 405  
..... Project 8-23-02-003

Investigation of ..... PHOTOREMISSIVE SURFACES.....

Subject of Report ..... Progress Report for Period.....  
..... April 1 to July 1, 1952

Submitted by ..... R. W. Lassettre.....

Date..... September 12, 1952

**UNCLASSIFIED COPY**  
FOR INFORMATION ONLY

During the period April 1 to July 1 the same personnel were involved as in the previous period. Research has continued along three lines: (1) study of development of photosensitivity on cesium addition, (2) study of photocathode composition, and (3) study of structures of cesium oxides. The chief results are summarized in the next section and several experiments are then described in more detail.

### SUMMARY

In the last progress report an account was given of several experiments in which cesium was slowly added to an oxidized silver sheet and thermionic emission measured continuously during the process. Two maxima in thermionic emission were found, and phototubes were prepared at each of several stages. The results indicated (1) that the rate of reaction in the solid phase of the cathode was slow, (2) the best photocathodes were obtained if the cesium addition was stopped near the second maximum, and (3) not all of the higher cesium oxides ( $\text{Cs}_2\text{O}_3$ ,  $\text{CsO}_2$  etc.) were converted to  $\text{Cs}_2\text{O}$ .

During the present quarter this study has been continued. Very small capillaries have been used to limit the cesium flow rate, and in addition, photoelectric emission has been followed continuously during cesium addition by means of a set of infrared filters. The capillary diameters and lengths have been measured so that cesium flow rates could be calculated, and hence the composition could be followed as a function of the time. As reported previously, two maxima in thermionic emission are found. Two corresponding maxima in photoelectric emission are also found, but the thermionic and photoelectric yields are not proportional. Subject to some qualification discussed in the next section, the gross Cs/O atomic ratio is less than 2.0 throughout the time range for which the infrared response

is appreciable. Thus at the maximum thermionic emission the cesium content is significantly less than that corresponding to  $\text{Cs}_2\text{O}$ . This tends to support the idea, previously advanced, that  $\text{Cs}_2\text{O}$  is not the only oxide in the photocathode at equilibrium although it must be the one present in major amount as the x-ray work previously reported establishes.

By cooling the cesium source, and thus effectively stopping the cesium flow at various stages, some further information concerning the mechanism of reaction has been obtained. In the early stages of fabrication, interrupting the cesium addition, leads to an immediate drop in both thermionic emission and infrared response. In the neighborhood of the first maximum, interruption of cesium flow causes a marked increase in emission to a maximum followed by a decrease. As the second maximum in the thermionic emission is approached, interruption of cesium flow again leads to an increase in emission, but the subsequent decrease is now slow. Slightly beyond the second maximum, interruption of flow leads to increase of emission to a stable maximum, no subsequent decrease being observed. These observations are accounted for if we assume the reaction to be diffusion controlled, the diffusion occurring, perhaps, through a layer of  $\text{Cs}_2\text{O}$ . On this layer, another layer of unreacted cesium accumulates. If this cesium layer is too thick or too thin, the work function is high and emission is low. Thus in the early stages where the  $\text{Cs}_2\text{O}$  layer is thin, reaction is rapid and only a thin cesium layer forms. On cooling the source, this cesium layer becomes even thinner and emission drops. As reaction proceeds, the  $\text{Cs}_2\text{O}$  layer becomes thicker and the reaction rate is less, thus permitting a thicker cesium layer to develop, and at some stage this thickness exceeds that corresponding to minimum work function. Beyond this point, interruption of cesium flow is accompanied by further reaction

which reduces the cesium film thickness. Since this thickness now passes through that of minimum work function, a maximum in emission occurs. At a still later stage the  $\text{Cs}_2\text{O}$  layer becomes so thick that decline from the maximum is not detected during the time of observation. This may be due to the fact that there is still just enough cesium flow to balance the reaction rate. A more likely explanation is that only a fraction of a monolayer of cesium is required for minimum work function and the reaction rate is proportional to the surface concentration of cesium. As the surface concentration is reduced the reaction rate falls to such a low value that it is no longer perceptible in these experiments. This model seems quite plausible and is in accord with the results of other investigators. That  $\text{Cs}_2\text{O}$  is the rate limiting layer is also plausible both because its presence is established by x-ray investigation and also because no suboxide of cesium ( $\text{Cs}_3\text{O}$  etc.) is stable at the temperature of these experiments ( $190^\circ\text{C}$ ). This mechanism seems plausible, but further experiments are continuing in order to test further the hypotheses. The experimental basis for this mechanism is discussed in section B.

Two further points are of interest. In the first place much evidence has accumulated which shows the pronounced influence of extremely small amounts of cesium on the infrared response. The effect is especially marked at room temperature, since the reaction rates are then too small for readjustment to occur. Contamination of the photocathode by excess cesium at room temperature results in a marked loss in photosensitivity, especially in the infrared. This can usually be reversed by heating the tube. The second point of interest concerns the effect of temperature on photoelectric yield. As the temperature is lowered from  $190^\circ\text{C}$  to room

temperature, the yield increases markedly, especially in the infrared. Factors of two or more are common. This is reversed on reheating the tube. Although this behavior has been repeatedly observed on cathodes fabricated in this laboratory, the phenomenon is apparently not of general occurrence since commercial cathodes are only slightly changed in response heating. The phenomenon is not clearly understood at present.

The determination of photocathode composition by radioactive tracers has progressed fairly rapidly. Silicon - cesium chromate mixtures, which produce cesium on heating, have been made containing radioactive cesium tracer, and means for accurately determining the tracer content have been worked out. Several experiments have been performed in which the cesium content of the photocathode has been determined. The Cs/O atomic ratio for the best phototubes is invariably less than corresponds to  $\text{Cs}_2\text{O}$ . The results are not yet firmly established because the quality of photocathode is quite variable. Some have lower infrared sensitivity than is expected on the basis of previous experience in the fabrication of similar cathodes, so further work is required. Other questions concerning cathode sputtering have also been raised which must be settled before the conclusions become firm. The radiotracer method itself is, however, quite simple and effective. The problems arise in phototube fabrication. One result of interest, which seems firmly established, is the rather large amount of cesium which appears on the glass walls. A blank glass disc, with the same area as the photocathode is used to protect the cathode back from radioactive tracer. This disc has, after processing, an activity of about 10% of the cathode. Since the total area of glass envelope is considerably greater than the cathode area, a considerable fraction of cesium (about half in some experiments) goes to the envelope. This fact is of considerable



interest for tube fabrication, because the distillation of even a tiny fraction of this cesium to the cathode at room temperature would result in a marked loss in photosensitivity. Whether the cesium on the walls is merely adsorbed or whether it has reacted with the walls to form an oxide or other compound is not known at present. The composition investigation is continuing.

The crystal structure of  $\text{Cs}_2\text{O}$  has been further refined by means of more careful intensity measurements, introduction of temperature corrections and other refinements. Using the experimental intensities, a Fourier projection of electron density has been computed and seems to indicate some polarization of  $\text{Cs}^+$  in the crystal field.

Several experiments are discussed in more detail in the following sections.

#### B. DEVELOPMENT OF THERMIONIC AND PHOTOELECTRIC EMISSION

By modifications in the experimental equipment and in the fabrication procedure, it has been possible to record continuously the thermionic emission and to determine periodically the response of the cathode to light transmitted through a series of filters. The experimental details of this investigation are presented in the following section. Because of the reproducibility of the results, the complete data for each cathode prepared are not presented, but rather the results are discussed in terms of the phenomena investigated and observed.

#### Experimental

To investigate conveniently the development of the thermionic and photoelectric emission during cesium addition, it was necessary to make

several modifications in the equipment and in fabrication procedure for the preparation of massive cathodes. A schematic drawing of the equipment used during the formation of the final photosurface is shown in Fig. 1.

The thermionic emission during the fabrication was continuously measured using the vibrating reed amplifier coupled to the Brown recorder. The input resistance to the vibrating reed may be varied from  $10^3$  to  $10^8$  ohms by powers of 10. This permits the recording of currents from  $4.55 \times 10^{-9}$  to  $4.2 \times 10^{-4}$  amperes full scale recorder deflection. The thermionic and photoelectric emission data are reported as millimeters of recorder deflection on the  $10^5$  ohm input resistor range for which the sensitivity is  $0.15 \mu\text{a/mm}$ .

The photoelectric emission characteristics of the cathode during the cesium addition are measured by illumination of the cathode with light from a G.E. No. 31, 6.2-volt bulb, passed through a series of filters. The light filter carrier and the bulb are mounted in a two-inch diameter brass tube which passes through a hole in the door of a Cenco No. 95050 oven. The experimental tube was mounted with the cathode in the light beam as shown in Fig. 1. During the cesium addition the tube was periodically illuminated by the light transmitted through the filters, and the photoelectric current was measured on the Brown recorder using the thermionic emission as the base line. With the light source used, the photoelectric response was always large enough to be readily measured.

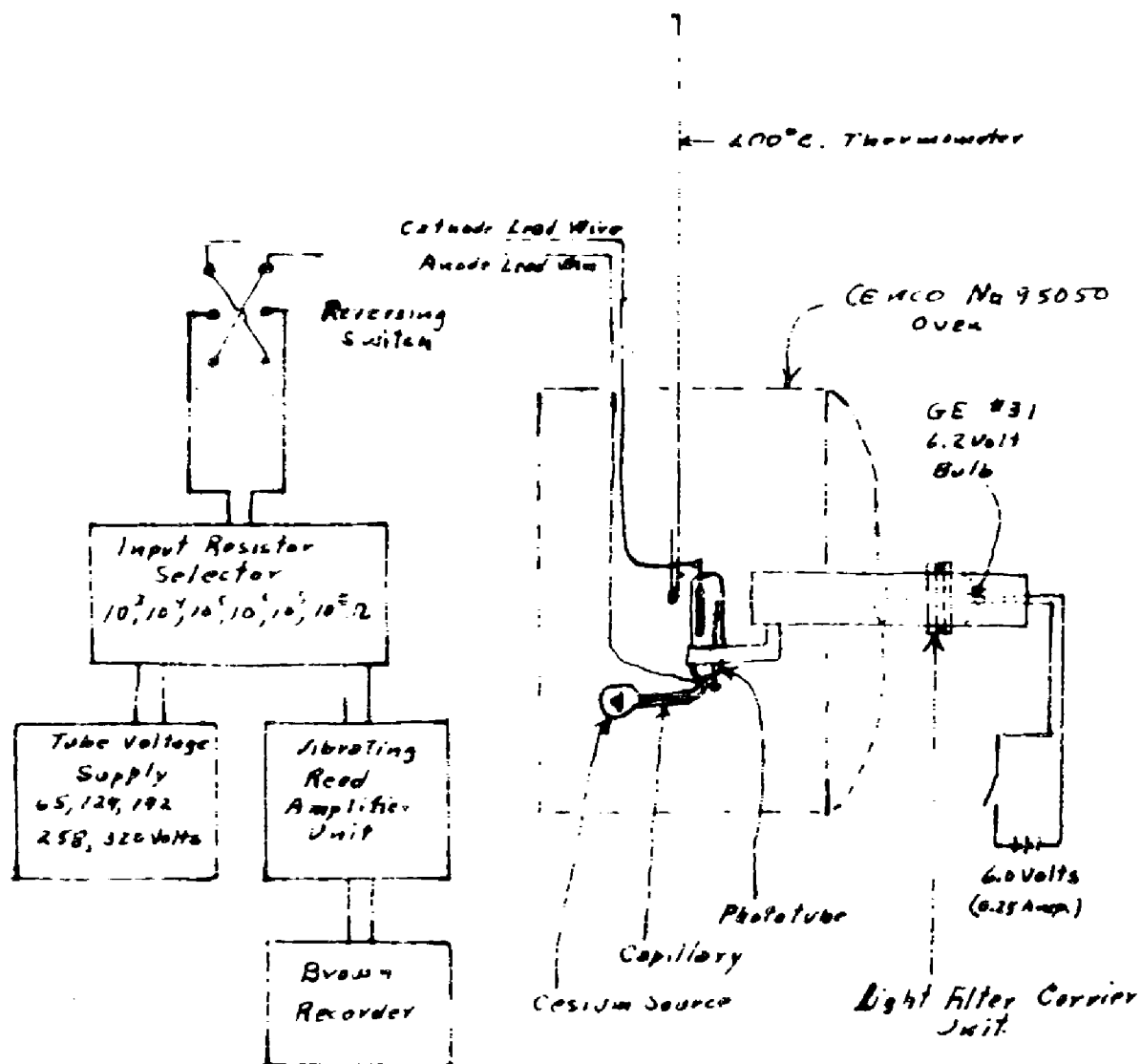


Fig. 1 Experimental Tube Preparation Equipment

The five filters used in the investigation were

F1 - clear glass

F2 - Polaroid XKA-60  $\lambda > 775 \text{ m}\mu$

F3 - Polaroid XKA-30  $\lambda > 830 \text{ m}\mu$

F4 - Corning 2540  $\lambda > 800 \text{ m}\mu$

F5 - Polaroid XKN-14  $\lambda > 880 \text{ m}\mu$

The spectral response of a 1P25 phototube, determined by passing the light beam from the Beckman DU spectrophotometer through the corresponding filters is shown in Fig. 2. In this figure it is worth noting that the F2 response measures the infrared response beyond  $775 \text{ m}\mu$  without introducing a large absorption correction for wave lengths beyond  $900 \text{ m}\mu$ . In addition, a cathode which has an appreciable response beyond  $900 \text{ m}\mu$  must have a fairly large F5 response. Thus the ratio  $F2/(F1-F2)$  may be used as an approximate measure of the infrared response relative to the visible spectrum response.

The procedure for the preparation of a tube was modified in the following manner. After the oxidation and the firing of the cesium pellet in the side tube, the tube was tipped off the vacuum system. It was then mounted in the tube holder attached to the door of the  $190^\circ\text{C}$  oven, the cathode being in position to receive the light beam from the filter system. The leads to the vibrating reed amplifier were connected to the tube and the oven door was closed. As the tube was heated to  $190^\circ\text{C}$  and cesium was added through the capillary, the thermionic emission was continuously recorded and the photoemission was periodically measured.

The rate of the cesium addition during the tube preparation was determined by the flow characteristics of the capillary connecting the cesium

Fig. 2

Spectral Response of IP25  
Determined with Filters in  
the Incident Light Beam.

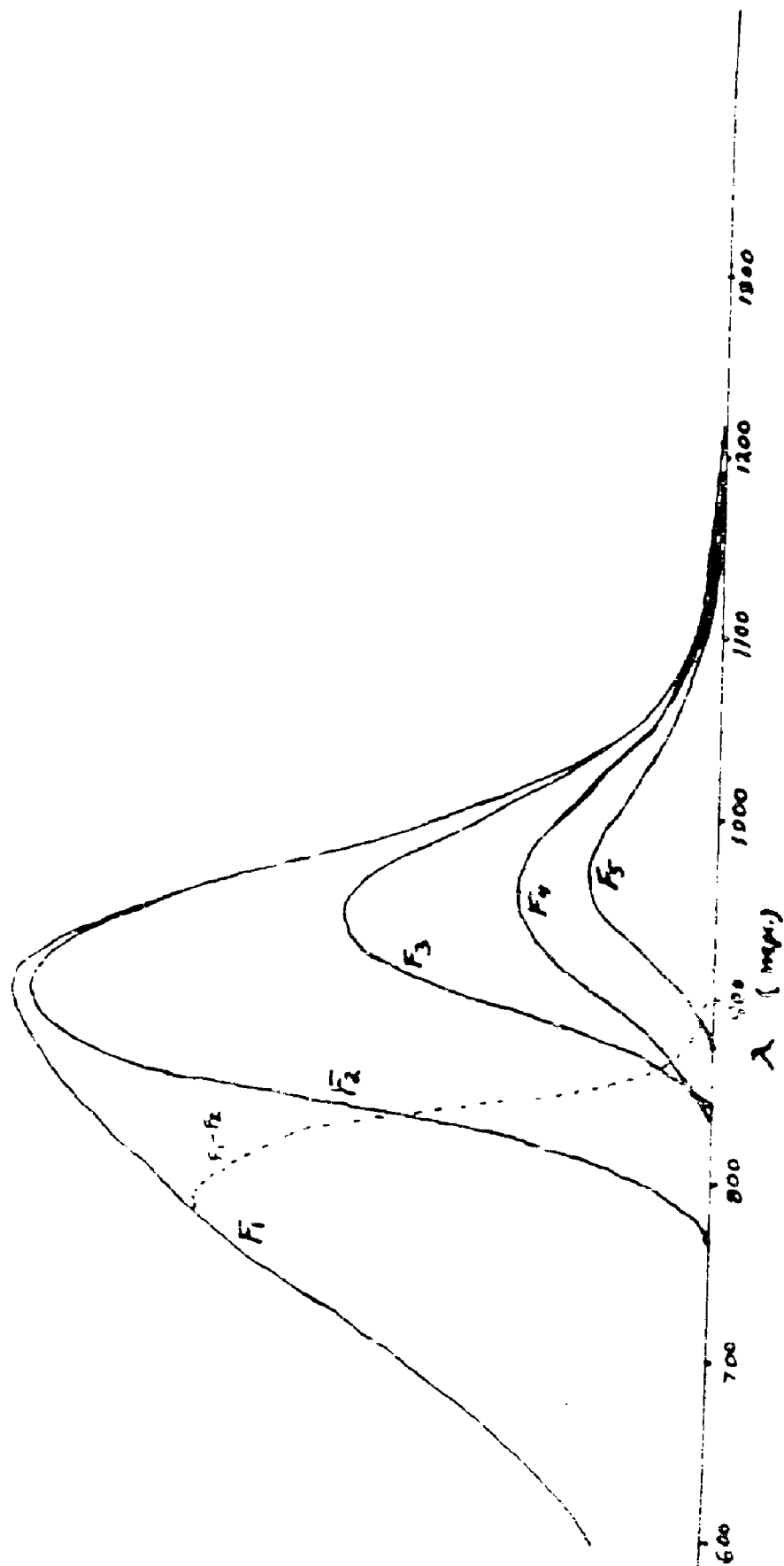
F<sub>1</sub> - Plate Glass

F<sub>2</sub> - Polaroid KRX-60

F<sub>3</sub> - Polaroid XRN-30

F<sub>4</sub> - Corning 2540

F<sub>5</sub> - Polaroid XRN-14



source to the tube. The cesium flow rate for the capillary was computed using the equation for free molecule flow:<sup>1</sup>

---

I. S. Dushman, Vacuum Techniques. John Wiley and Sons, Inc., N.Y., N.Y. (1949) p. 96.

---

$$n(\text{moles/sec}) = 3636 \pi^{\frac{1}{2}} A \sqrt{\frac{\pi}{M}} \left( \frac{P}{RT} \right)$$

$$n_{\text{Cs}}(\text{moles/sec}) = 1.589 \frac{a^2 \pi^{\frac{1}{2}}}{\sqrt{T}} P_{\text{mm}} \times 10^{-2}$$

where

$$K^{\frac{1}{2}} = \left( 1 + \frac{3}{8} \frac{l}{a} \right)^{-1}$$

$l$  = length of capillary, cm.  
 $a$  = radius of capillary, cm.  
 $P$  = vapor pressure of Cs in source  
 $A$  =  $\pi a^2$   
 $M$  = atomic wgt. of Cs = 132.91  
 $R$  = 62.36 mm. liter deg<sup>-1</sup> mol<sup>-1</sup>  
 $T$  = absolute temperature, °K

The vapor pressure of the cesium in the source was computed using the equation given by Dushman<sup>2</sup>

---

2. ibid p. 745

---

$$\log P_{\mu} = 9.66 - \frac{3774}{T}$$

where  $P_{\mu}$  is the vapor pressure in microns and  $T$  the absolute temperature.

During the fabrication of the cathode at 190°C. it was of interest to investigate the effect of stopping the cesium addition at various stages in the processing. This was accomplished by momentarily opening the oven door, placing a piece of cotton saturated with water on the cesium source, and then closing the door. The cesium vapor pressure in the source was thus reduced from 92.1 microns at 190°C to less than 0.065 microns, the vapor pressure at 100°C. This effectively stopped the cesium addition.

In the preparation of the cathodes it was highly desirable to reproduce the tube geometry as closely as possible. Consequently the same cathode was used in the preparation of PT 46, 47, 48 and 49. After each run the tube seal-offs were opened and the surface and tube envelope cleaned by washing with 6N HNO<sub>3</sub> followed by rinsing with distilled water. For the tubes PT 46, 47, and 48, the same capillary was also used, so that for these three tubes the actual cesium flow rates were identical.

The variables which were investigated using the massive cathode tubes were as follows:

1. PT 44 TE Development of thermionic emission with a constant rate of cesium addition.
2. PT 46 TE Development of thermionic and photoelectric emission with a constant rate of cesium addition. The cesium source was cooled once during the run.
3. PT 47 TE Variation of the thermionic and photoelectric emission with cooling of the cesium source. Cathode oxidized to a brilliant green,  $1.71 \times 10^{-5}$  mole of O.
4. PT 48 TE Similar to PT 47 TE. Cathode oxidation barely perceptible,  $0.938 \times 10^{-5}$  mole of O.
5. PT 49 TE Similar to PT 47 TE. Cathode oxidized to a black color,  $3.5 \times 10^{-5}$  mole of O. Cesium flow rate increased from  $7.2 \times 10^{-8}$  to  $38.8 \times 10^{-8}$  mole per minute.

Pertinent data for the fabrication of these cathodes are presented in Table 1. The times given for the deposition of a cesium monolayer on the cathode at 190° and 100°C were computed by assuming a cathode area of 21.1 cm<sup>2</sup>, a cesium atom radius of 3.0Å, cubic packing of the cesium on the surface, and the calculated cesium flow rate.

Table 1

## Experimental Tube Data

	Tube				
	44	46	47	48	49
Oxygen (Atom Mol. $\times 10^5$ )	1.30	1.35	1.71	0.938	3.5
Cs (190 °C. Moles/Min $\times 10^6$ )	15.1	7.2	7.2	7.2	38.8
Time for Cs Monolayer 190 °C (Min.)	0.064	0.133	0.133	0.133	0.0248
Time for Cs Monolayer 100 °C (Min.)	49	103	103	103	19.2
1st. Max. Thermionic Emission ( $\text{mm} \times 10^5$ Range)	345	420	320	480	--
2nd. Max. Thermionic Emission ( $\text{mm} \times 10^5$ Range)	550	870	2300	2000	525
Cool Cs Max Thermionic Emission ( $\text{mm} \times 10^5$ Range)			5700	5450	1600
Final Photosens. (F2/F1)		0.158	0.614	0.512	0.555
Final Photosens. (F5/F1)		0.004	0.148	0.102	0.128
Final Photosens. Peak $\lambda$ ( $\mu$ )			970	950	920
Final Photosens. long $\lambda$ limit			>1500	1550	1300
Final Photosens. $\frac{1}{2}$ max current $\lambda$			1075	1085	1015

Discussion of Results

The investigation of the effect of the cesium addition on the thermionic and photoelectric emission has demonstrated that the general characteristics of the massive cathode during fabrication at 190 °C are reproducible. Therefore, to avoid unnecessary repetition of the data, the results are presented in terms of the phenomena investigated.



### Composition and Thermionic Emission

Throughout the fabrication of PT 44 TE the cesium addition rate was constant at 190°C. Consequently, for this cathode, the gross composition within the tube may be expressed in terms of the Cs/O mole ratio using the calculated cesium flow rate and the observed amount of oxygen deposited during the oxidation. The cesium flow rate in moles per minute after correction for the initial heating to 190°C is

$$n_{Cs} = 7.8 \times 10^{-7} + 7.2 \times 10^{-8} (t - 24)$$

where  $t$  is the time in minutes. Since  $1.35 \times 10^{-5}$  gram atomic weight of oxygen was deposited during the oxidation, the Cs/O mole ratio after 24 minutes is

$$(Cs/O) = 5.33 \times 10^{-3} t - 7.03 \times 10^{-2}.$$

The thermionic emission of PT 44 TE as a function of time and the (Cs/O) mole ratio is shown in Fig. 3. The character of the current being measured was determined by measuring the current as a function of voltage. During the first 80 minutes and beyond 200 minutes the current was proportional to the voltage corresponding to an ohmic conduction current. In the region between 90 and 190 minutes the voltage-current relationship exhibited a saturation effect corresponding to thermionic emission.

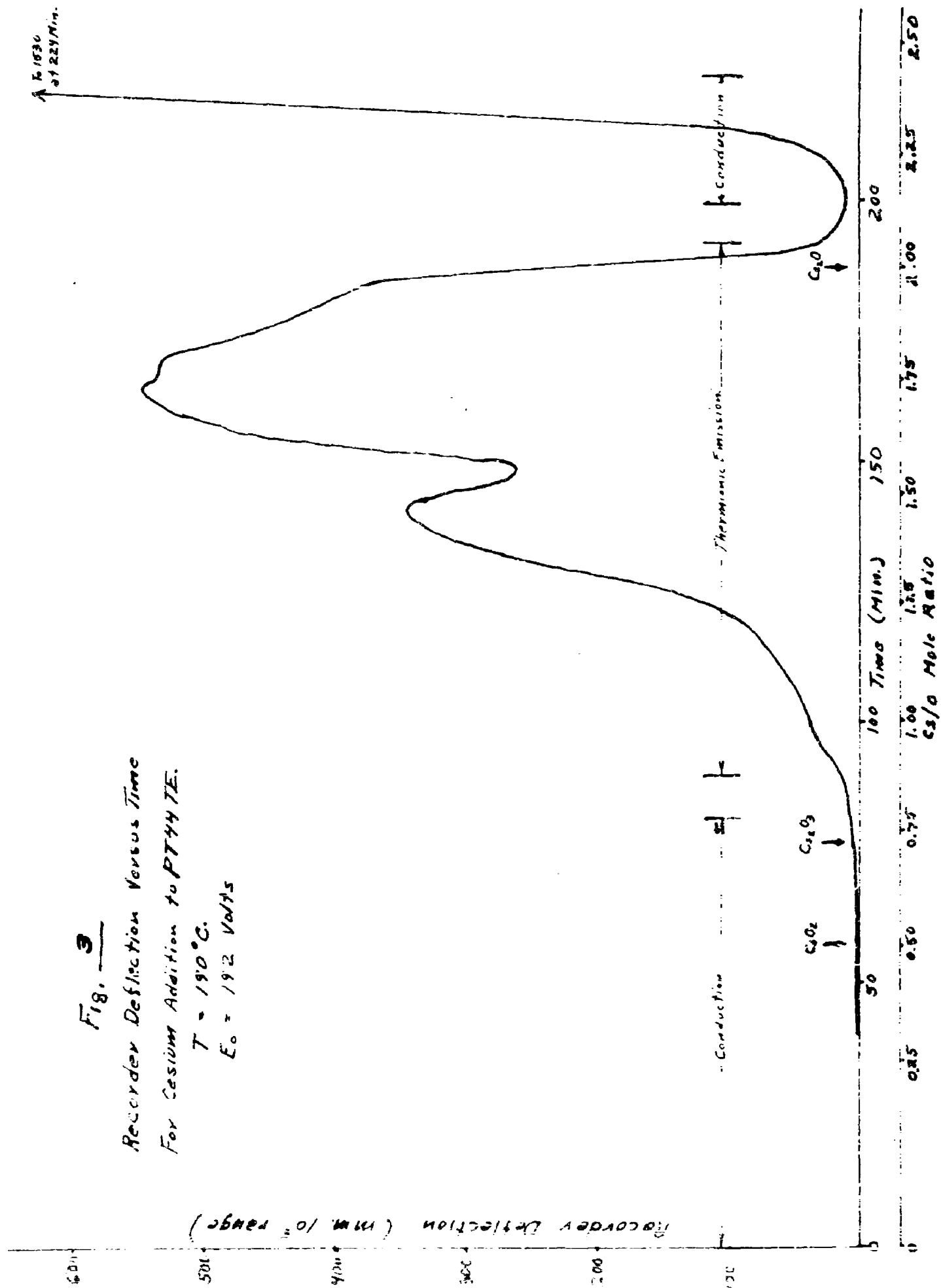
The thermionic emission versus time curve for PT 44 TE has two maxima. The first maximum appears at 141 minutes where the Cs/O ratio is 1.46, and the second maximum, at 164 minutes, occurs at a gross Cs/O ratio of 1.71. The rapid decrease in the thermionic emission between 150 and 190 minutes extrapolates to zero thermionic emission at Cs/O equal to 2.03. For the series of tubes the first thermionic emission maximum was observed to occur at  $0.8 \pm 0.05$  of the time required to reach the second maximum.

Fig. 3

Recorder Deflection Versus Time  
For Cesium Addition to PT44 TE.

$T = 190^{\circ}\text{C.}$

$E_0 = 19.2 \text{ Volts}$



In the figure it is interesting to note that the thermionic emission did not appear to a significant degree until the gross composition was beyond  $\text{Cs}_2\text{O}_3$ . Furthermore, the conduction current associated with excess cesium did not increase rapidly until the composition  $\text{Cs}_{2.25}\text{O}$  was passed. According to the phase diagram the equilibrium phases at  $190^\circ\text{C}$  as cesium is added to oxygen are  $\text{O}_2(\text{g}) - \text{CsO}_2(\text{s})$ ,  $\text{CsO}_2(\text{s}) - \text{Cs}_2\text{O}_3(\text{s})$ ,  $\text{Cs}_2\text{O}_3(\text{s}) - \text{Cs}_2\text{O}(\text{s})$ , and  $\text{Cs}_2\text{O}(\text{s}) - \text{Cs}_{2.9}\text{O}(\text{l})$ . Thus if the system were at equilibrium the liquid phase cesium saturated with oxygen ( $\text{Cs}_{2.9}\text{O}$ ) would not appear until the  $\text{Cs}_2\text{O}$  composition is passed. A priori, it would be anticipated that as the surface of  $\text{Cs}_2\text{O}$  was covered with excess cesium the thermionic emission would rapidly decrease as the work function was increased toward the value for cesium. Actually the thermionic emission is observed to decrease before the calculated  $\text{Cs}_2\text{O}$  composition is passed.

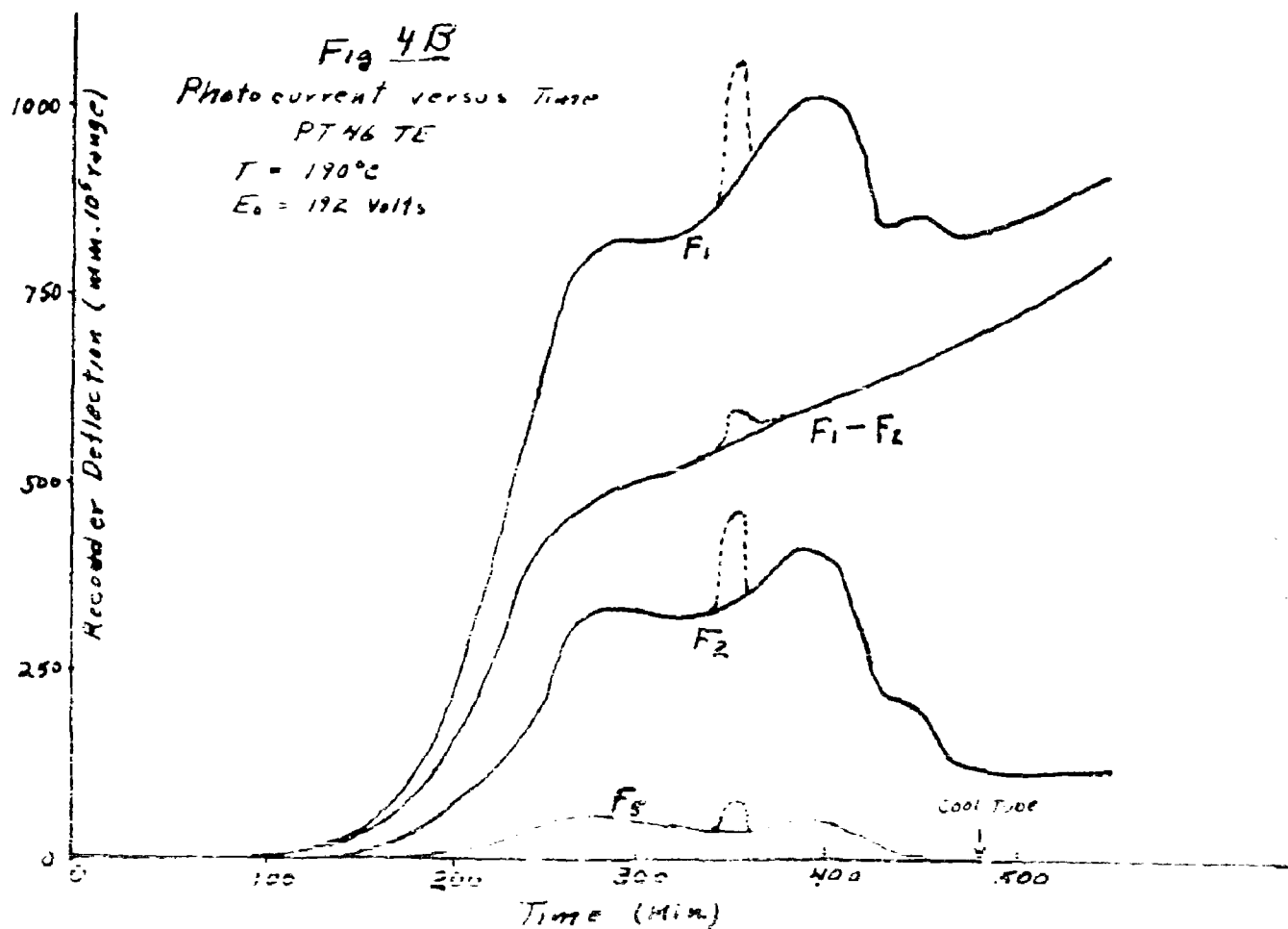
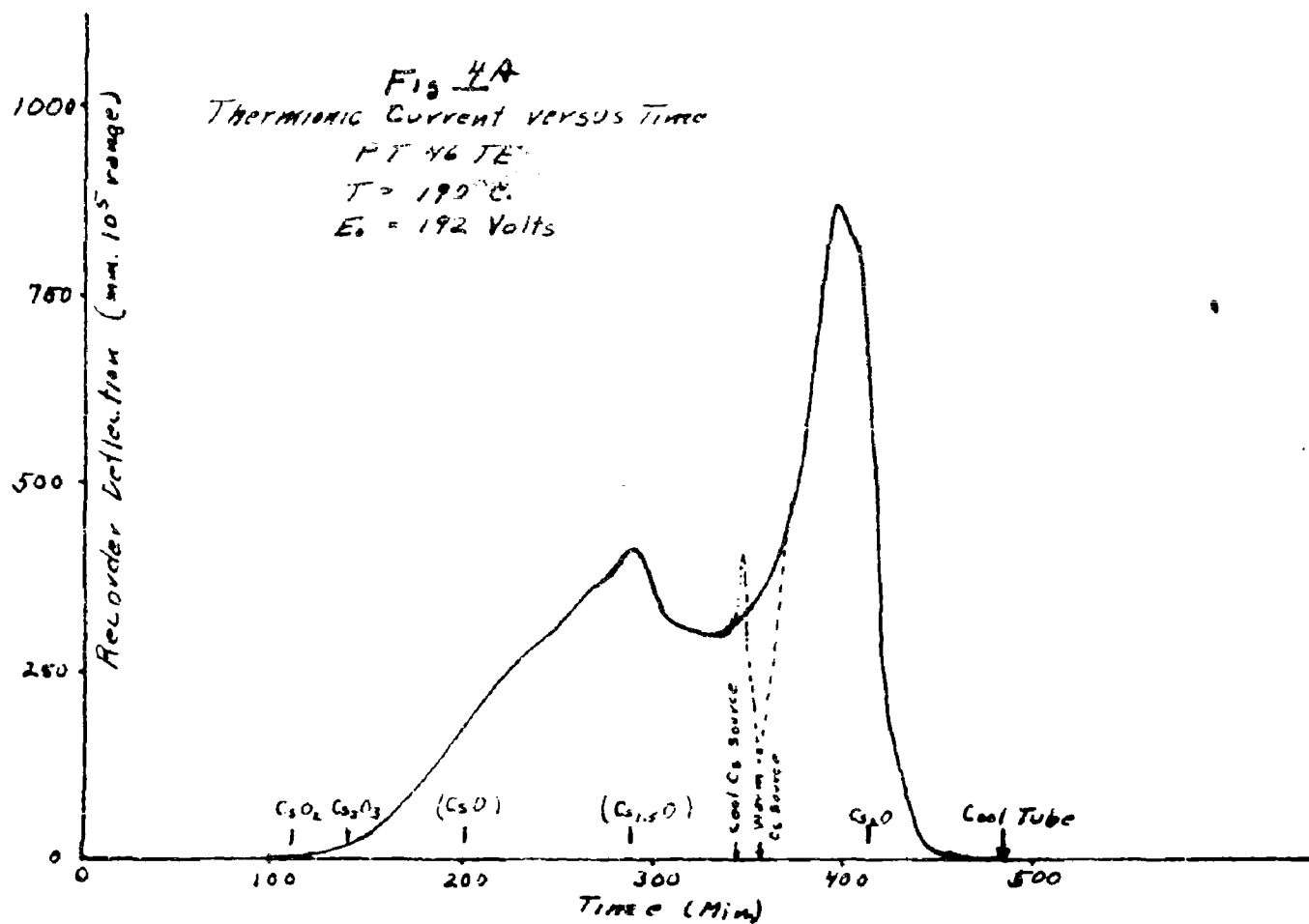
Though the compositional data are consistent with the chemical properties of the cesium oxides, there exists considerable uncertainty in the actual (Cs/O) mole ratio for the cathode. The amount of oxygen deposited during the oxidation is known only to  $\pm 5\%$ . The actual vapor pressure and molecular weight of the cesium are not accurately known for the experimental temperature range. The equation used to calculate the cesium vapor pressure was determined by a positive-ion method and consequently is the vapor pressure in terms of cesium atoms, without considering the equilibrium distribution of cesium between  $\text{Cs}_2$  and Cs. Consequently the actual flow rate in atoms per minute could be less by a factor of  $\sqrt{2}$  if the cesium were present as  $\text{Cs}_2$ . In addition to the above uncertainties the extent to which cesium is sorbed by the glass envelope of the tube is unknown. It is interesting that the major errors would tend to reduce further the actual (Cs/O) mole ratio on the cathode.

### Photoelectric Emission versus Time

The development of the photoelectric and thermionic emission during the cesium addition was investigated with tube PT 46 T2. In the preparation of this cathode the cesium rate was reduced to  $7.2 \times 10^{-8}$  mole per minute. With this rate, corresponding to the deposition of a cesium monolayer every 0.133 minutes, it was anticipated that the rate of the chemical reactions at the cathode would be rapid compared to the rate of cesium deposition. Thus the cathode surface would be at chemical equilibrium during the cesium addition. Actually this proved to be an invalid assumption.

The thermionic and photoelectric emission versus time data for PT 46 T2 are shown graphically in Figs. 4A and 4B. The thermionic emission curve is similar to the curve for PT 44 T2. The photoelectric emission for the series of filters exhibits two maxima coinciding with the time of appearance of the thermionic maxima. From the figures it is evident that the thermionic and photoelectric emissions during cesium addition do not exhibit a 1 : 1 correlation. The second maximum in thermionic emission at 395 minutes corresponds to twice the emission at the first maximum. The F5 infrared responses at the two peaks in thermionic emission, however, are equal. The F1 and F2 responses at the second maximum are slightly greater than at the first thermionic emission maximum.

During the preparation of this cathode the cesium source was cooled from 345 to 355 minutes by placing moistened cotton on the cesium source bulb. The thermionic emission immediately increased to a maximum and then decreased as indicated by the dotted curve in Fig. 4A. The photoresponse also exhibited a marked increase as shown by the dotted curve in Fig. 4B. Actually cooling the cesium source doubled the F5 infrared response. Considering the characteristics of the filters, the changes in spectral response



accompanying the cooling of the cesium source must correspond to a marked development of infrared sensitivity in the region beyond 880  $\mu$ . This behavior on cooling the cesium clearly demonstrates that the rate of the reactions at the surface actually is slower than the rate of cesium deposition.

The cesium addition to PT 46 TE was continued until the thermionic emission had decreased from 870 ( $\text{mm} \times 10^5$ ) range to 91  $\text{mm}$  on the  $10^8$  range. As cesium was added beyond the second maximum in thermionic emission, the infrared sensitivity steadily decreased while the visible (F1 - F2) response steadily increased. Cooling the cathode to room temperature resulted in an increase in the F1 response without any significant change in F2. This would indicate that the spectral response was increasing at wavelengths shorter than 775  $\mu$ .

#### Effect of Cooling the Cesium Source

The change in the thermionic and photoelectric emission when the cesium source is cooled was investigated during the fabrication of PT 47, 48, and 49. The general characteristics of the effects are best illustrated by the data for PT 47 TE.

In the preparation of PT 47 TE the cathode was oxidized to a brilliant green corresponding to the deposition of  $1.71 \times 10^{-5}$  gram atom of oxygen. The rate of cesium addition at 190°C was the same as for PT 46, namely  $7.2 \times 10^{-8}$  mole per minute. The calculation of the Cs/O ratio as a function of time was not attempted because of the uncertainties introduced by the periodic cooling of the cesium source.

The changes in the thermionic and photoelectric emission of PT 47 TE when the cesium source was cooled at various processing stages are shown in Figs. 5 and 6. In the thermionic emission region before the first

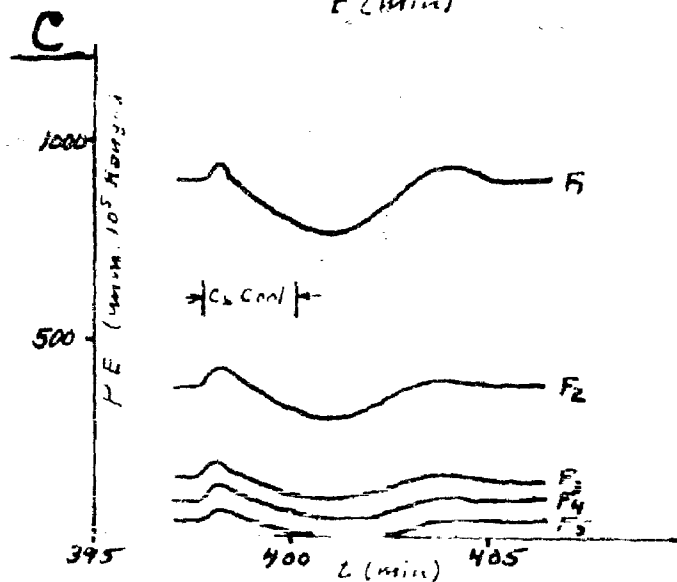
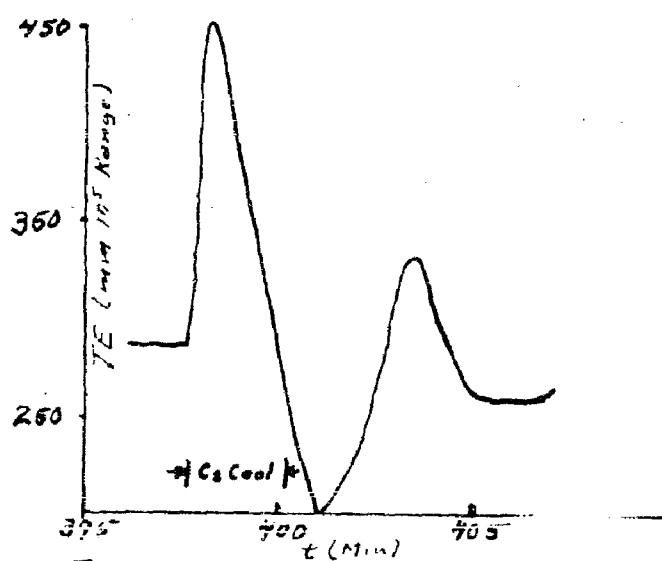
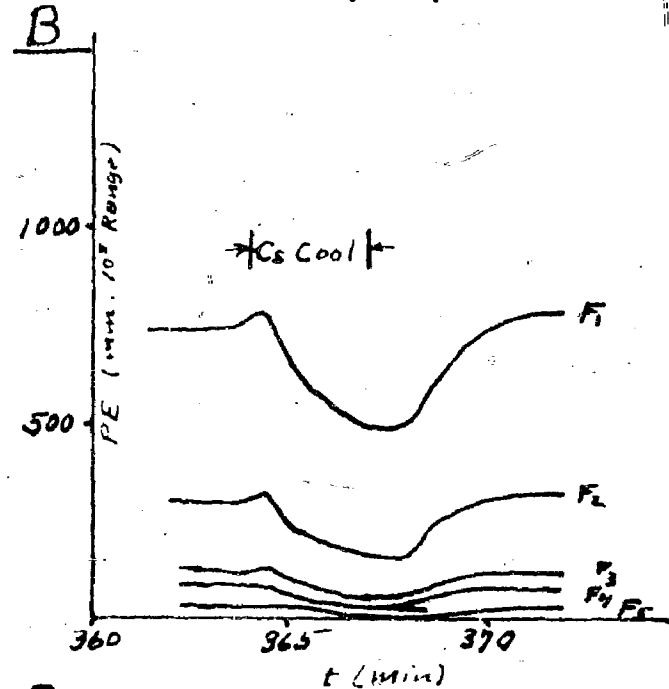
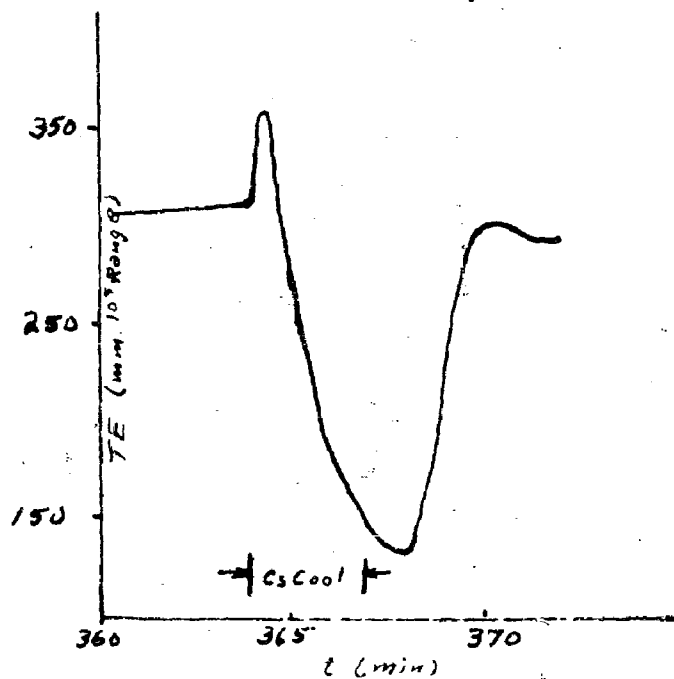
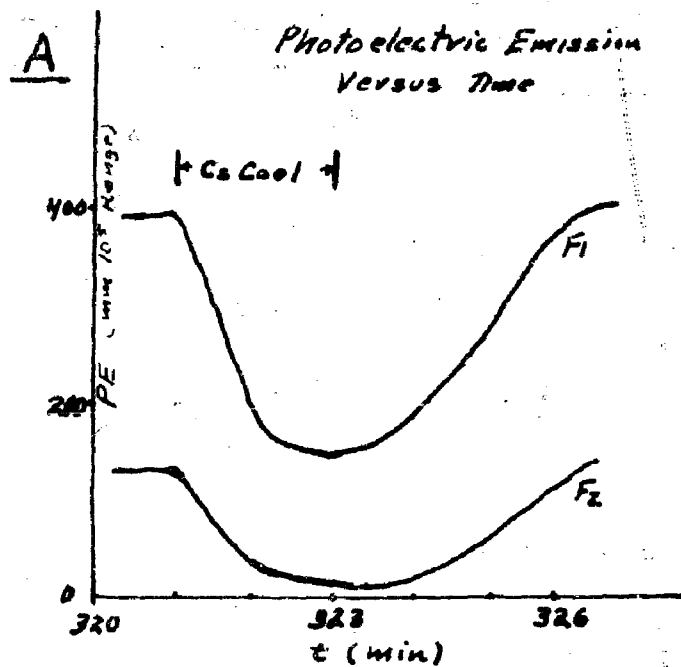
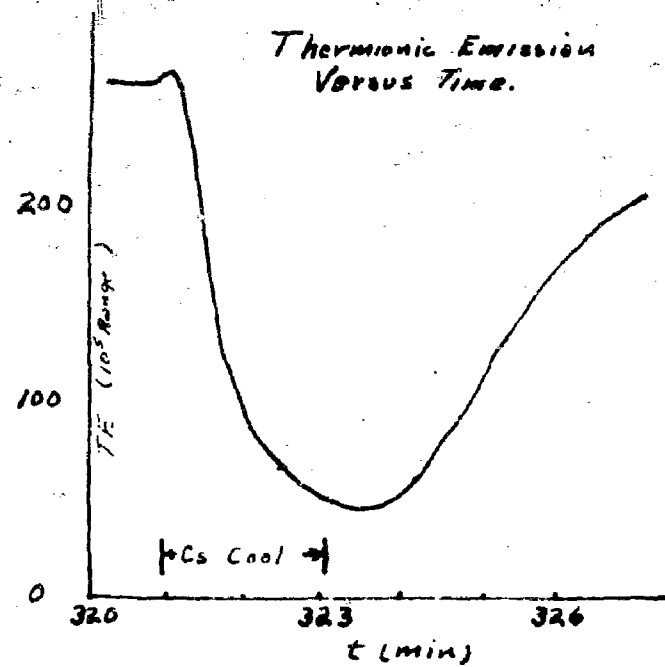
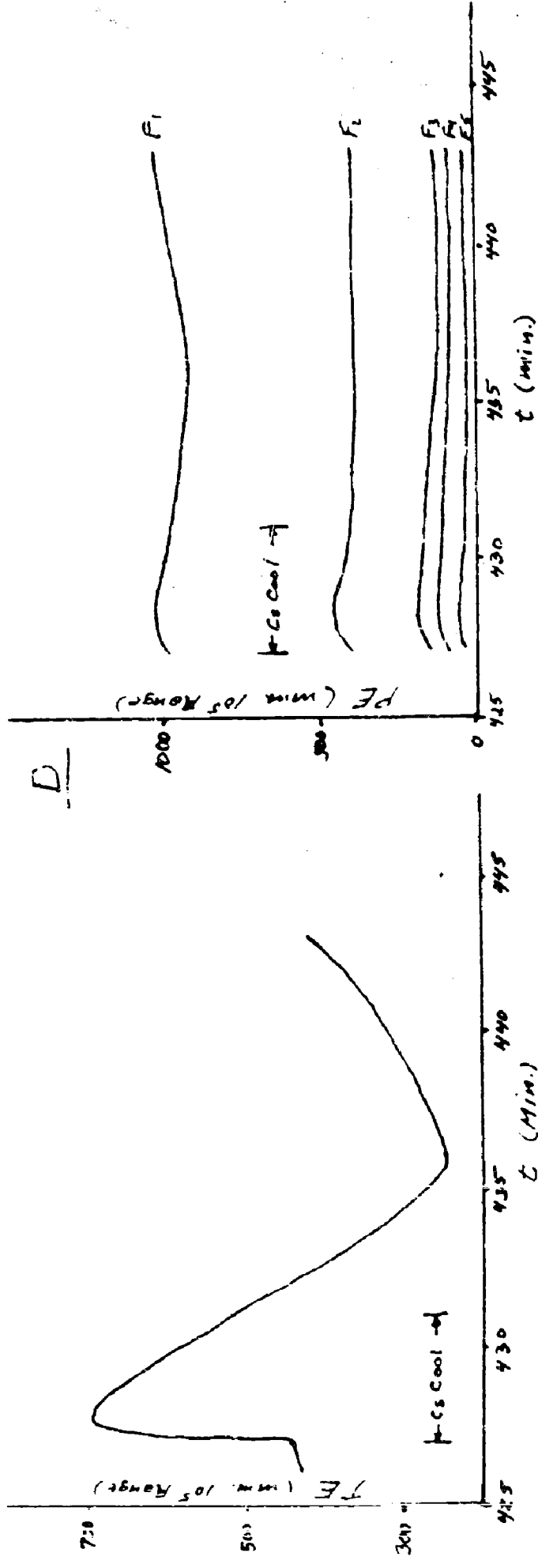


**Fig. 5** Effect of Cooling Cesium Source on Thermionic Emission (TE) and Photoelectric Emission (PE)  
 PT 47 TE,  $T = 190^\circ\text{C}$ ,  $V = 192\text{ Volts}$

D



E

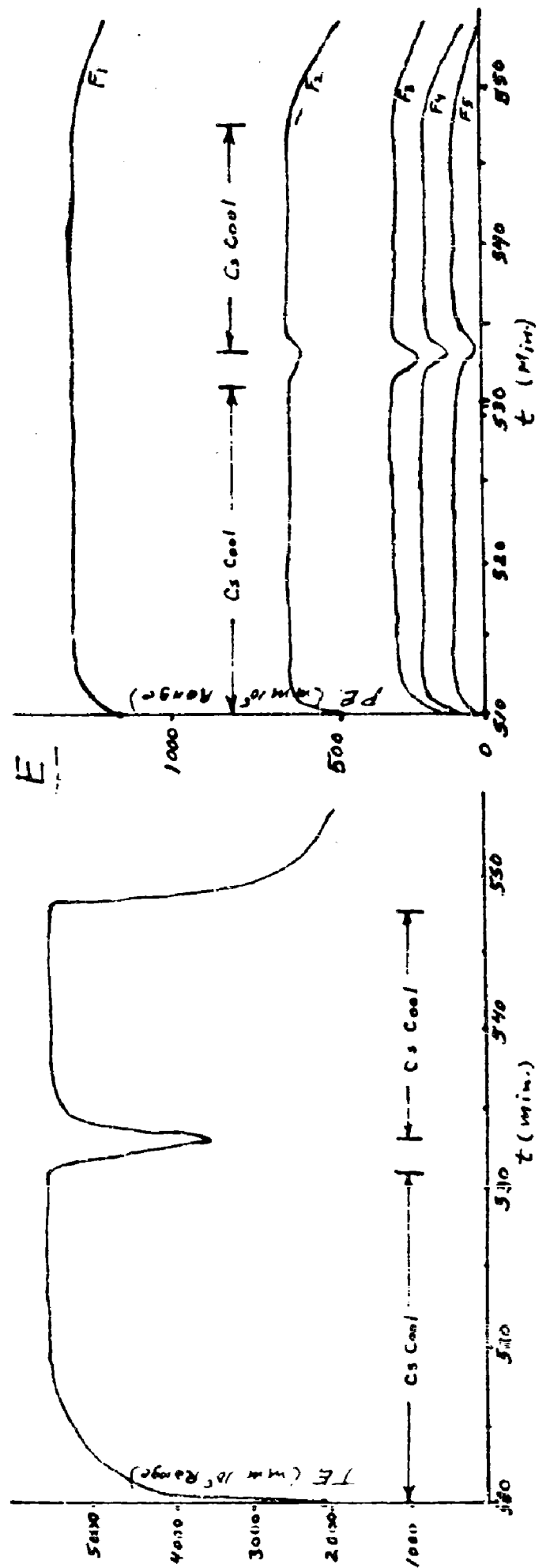


Fig. 6 Effect of Cooling Cesium Source on Thermionic Emission (TE) and Photoelectric Emission (PE)  
 PJ 47 TE,  $T = 190^\circ\text{C}$ ,  $E_0 = 19.2$  Volts



maximum, cooling the cesium source results in a rapid decrease in the thermionic and photoelectric emission as shown by Fig. 5A. As the first maximum is approached, cooling the cesium source results in an initial increase in both the thermionic and photoelectric emission, followed by a decrease to a value less than existed before cooling. Reintroducing cesium causes the emission to increase to a second maximum followed by a decrease to the original value observed before the cesium was cooled. In PT 47 TE the first maximum occurred at 395 minutes. Thus the curves in Figs. 5B and 5C illustrate the changes in thermionic emission in the region of the first maximum. It is of interest to note that corresponding to the decrease in thermionic emission, the infrared emission decreases without a marked change in the (F1 - F2) response. This suggests that there actually exist two photoelectron sources giving rise respectively to visible and infrared sensitivity, the latter being related to the thermionic emission.

As the second maximum in thermionic emission is approached, cooling the cesium source results in a rapid increase in the thermionic and photoelectric emission, followed by a slow decrease. The rate of decrease of emission beyond the peak value decreases on approaching the second maximum (compare Fig. 5C to Fig. 6D). Cooling the cesium source at 510 minutes (second maximum in thermionic emission at 500 minutes) resulted in an increase in the thermionic and photoelectric emission to a stable maximum value as shown in Fig. 6E. The momentary warming of the cesium source at 531 minutes produced an immediate decrease in the emission. Recooling the cesium source restored the emission to the original value. Considering that the calculated rate of cesium addition corresponds to the deposition of approximately 1.5 layers of cesium per minute with the cesium source at

190°C, the rapid rate of decrease in thermionic emission with warming of the cesium source is rather surprising. The cooling of the tube during the momentary opening of the oven door would contribute to this decrease; however, recooling the cesium source resulted in an immediate increase. Actually the time required to place the moist cotton on the cesium source is significantly longer than is required for its removal. Thus, the amount of cesium required to depress the emission of the "stable" surface at 190°C is very small. It is shown in Fig. 6E that this addition of cesium practically eliminates the F5 sensitivity; thus the long wavelength limit shifts toward the visible upon adding a small amount of cesium.

At 548 minutes the cesium addition was resumed, and within 2.5 minutes the thermionic and photoelectric emission had decayed to values less than existed at the second maximum in thermionic emission. The cesium addition was continued for approximately ten minutes and the cesium source re-cooled. The thermionic and photoelectric emission again increased to the maximum values, but at a slightly lower rate than at the previous cooling (10 minutes compared to 8 minutes to obtain maximum emission). The entire tube was finally cooled to room temperature, producing a further increase in the infrared sensitivity as discussed in the following section.

The variation of the thermionic and photoelectric emissions on cooling and rewarming the cesium source indicates that the chemical reactions involved in the removal of the cesium from the surface of the cathode are actually slow reactions. In Figures 5B and 5C the second maximum in the emission forced during the reintroduction of cesium probably corresponds to the surface composition passing through the critical composition associated with the initial maximum on cooling the cesium. Thus during the

decay after passing the maximum emission with the cesium source cooled, the cesium content of the surface is decreased below the optimum value for infrared emission. The fact that the (F1 - F2) response is not appreciably changed indicates that the major change is occurring at wavelengths longer than 900  $\mu$ .

#### The Effect of Temperature on Photoemission

After the thermionic emission and photoemission for PT 47 TE became stable at 190°C with the cesium source cool, the entire tube was quickly cooled to room temperature by opening the oven door. During the cooling process there was a very marked increase in the infrared response as shown in Fig. 7A. The F5 response ( $\lambda > 880\mu$ ) tripled when the cesium source was cooled at 190°C; cooling the tube to room temperature almost tripled the response again. During this process the F1 - F2 response did not significantly change, and thus during the cooling of this tube the changes in the photoemissive characteristics are occurring in the infrared region beyond 880  $\mu$ .

The tube PT 48 TE was prepared using the same tube and capillary used in the preparation of PT 47 TE. The amount of oxygen deposited during the oxidation, however, was decreased from  $1.71 \times 10^{-5}$  to  $0.938 \times 10^{-5}$  gram atom of oxygen. With this extent of oxidation the silver grain structure of the base was readily visible through the oxide coat. The tube was fabricated at 190°C, using the same procedure as in the preparation of PT 47 TE. After the second maximum in thermionic emission was passed, the cesium source was cooled and the thermionic and photoelectric emission increased to constant values at 190°C. The maximum thermionic emission was 5450 ( $\mu$  x  $10^5$ ) as compared to 700 ( $\mu$  x  $10^5$ ) range of PT 47 TE. Cooling the

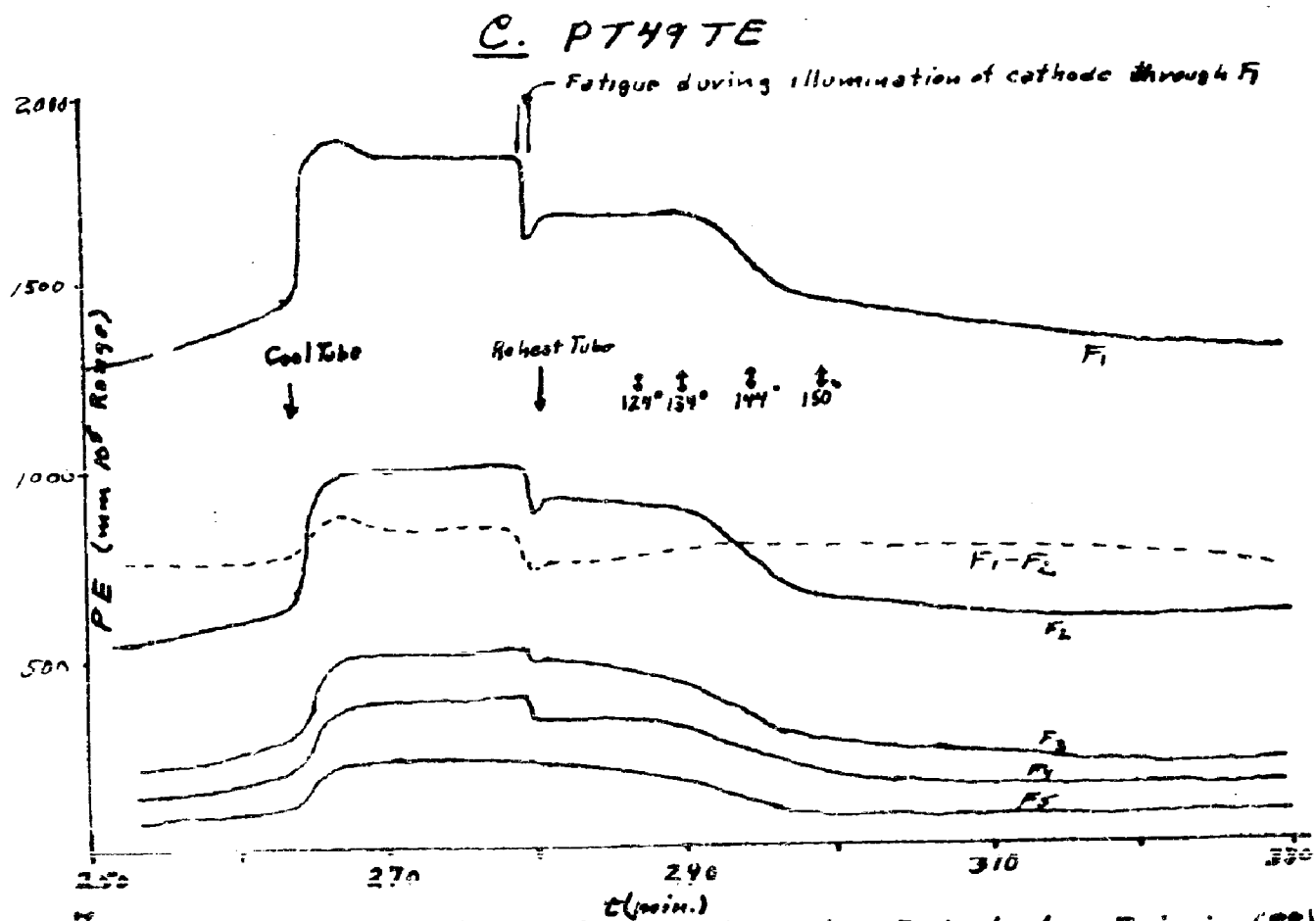
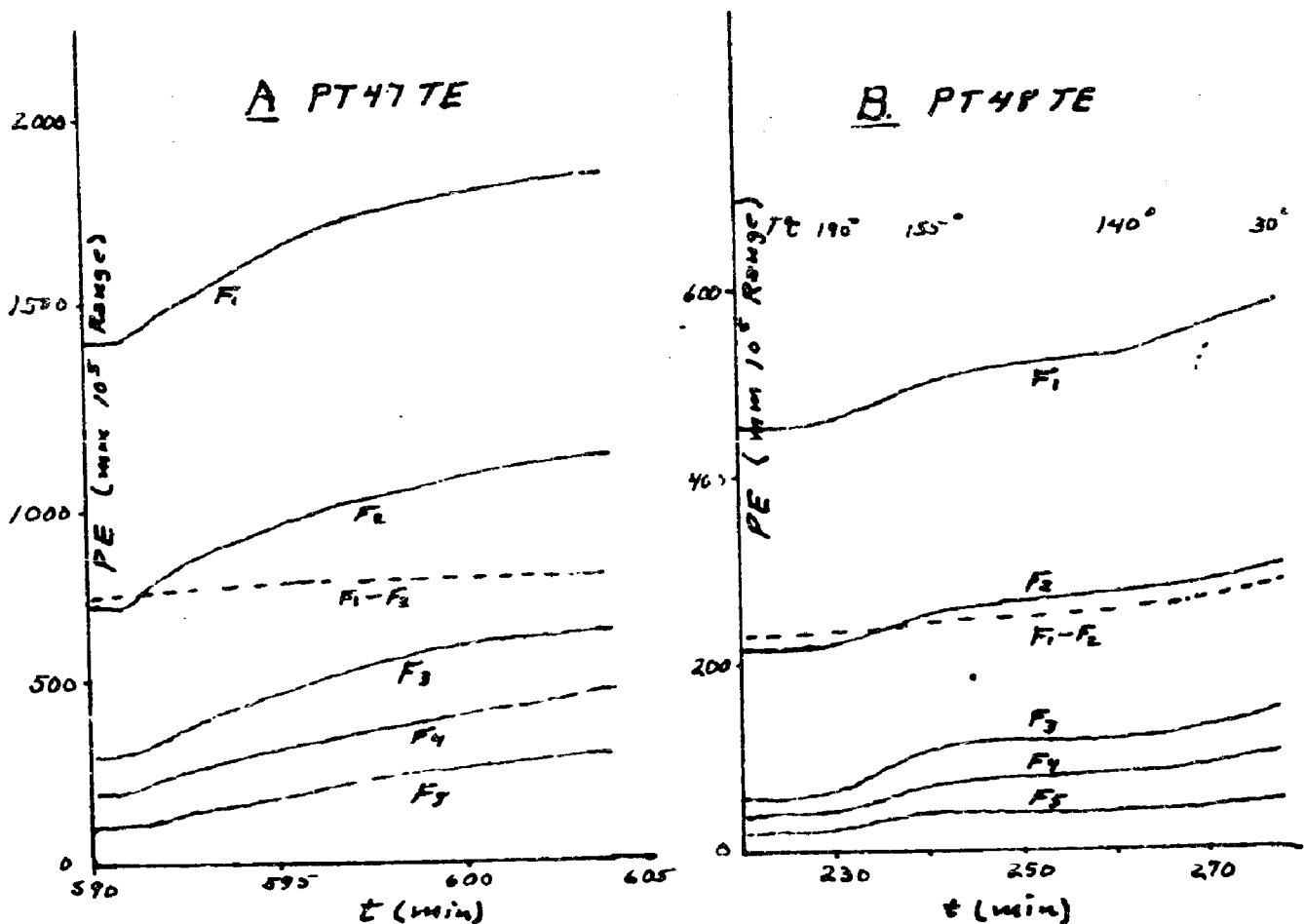


Fig. 1 Effect of Cooling tube from 190°C to 30°C on the Photoelectric Emission (PE)

source increased the thermionic emission from 2000 to 5450 ( $\text{mm} \times 10^5$ ) range, and the F2 response from 160 to 250 ( $\text{mm} \times 10^5$ ) range, with no appreciable change in the F4 and F5 responses. Thus in PT 48 TE, cooling cesium source modified the photoemission characteristics in the 775 to 880  $\text{m}\mu$  region.

After the emission with the cesium source cooled had stabilized at 190°C, the entire tube was cooled to room temperature. The cooling in this case was slowed down at 155°C by closing the oven door, the oven heater being set to control at 140 - 150°C. As shown in Fig. 7B a significant increase in the infrared response was obtained during the cooling to 155°C. Cooling the tube to 140°C in the oven resulted in slight increase in the F1 and F2 responses. The oven door was then opened and the tube cooled to room temperature. During this period there was a further increase in the response.

In the preparation of PT 49 TE the same cathode as for PT 47 TE was used but the oxygen content was increased from 1.71 to  $3.5 \times 10^{-5}$  mole of O, and the cesium flow rate was increased from  $7.2 \times 10^{-8}$  to  $38.8 \times 10^{-8}$  mole per minute. During the fabrication, the cesium source of PT 49 TE was cooled three different times after the peak in thermionic emission was passed. The peak during the cesium addition was 525 ( $\text{mm} \times 10^5$ ) range, and before the third cooling the emission had decreased to 150 ( $\text{mm} \times 10^5$ ) range. On cooling of the cesium source, the thermionic emission rapidly increased to 1250  $\text{mm}$ , with the F1 and F2 responses increasing from 870 to 1400 and 190 to 640 ( $\text{mm} \times 10^5$ ) range respectively. The entire tube was then cooled to room temperature at 264 minutes. The photoemission increased during cooling as shown in Fig. 7C. The surface at room temperature exhibited a "fatigue" effect on prolonged illumination through F1 and F2. This "fatigue"

effect produced the decreases in F1, F2, F3, and F4 sensitivity as shown at 279 minutes in Fig. 7C. There was a partial recovery of sensitivity during the dark period. The tube was then reheated to 190°C with the cesium source cold. During the heating period the photoemission remained relatively constant to 134°C. Between 134° and 150°C the photoemission decreased to the original 190°C. values. Thus the phenomenon of increasing photosensitivity on cooling from 190°C proceeds in a reverse direction during heating to 190°C.

#### Spectral Responses of Final Cathodes

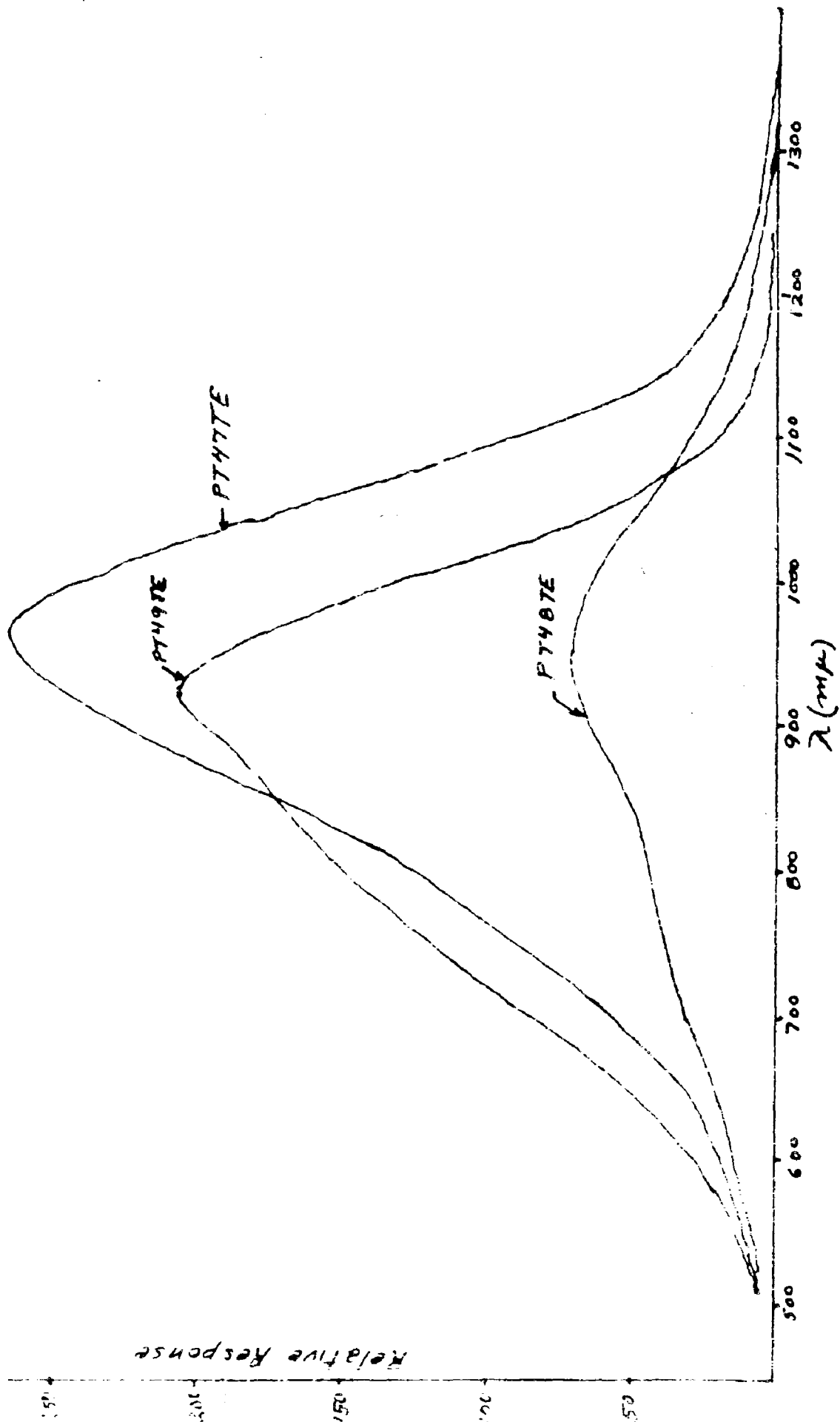
The Beckman DU spectrophotometer spectral responses of the tubes PT 47, 48, and 49 TE were measured after the tubes had been cooled to room temperature at the end of the run. The response characteristics, uncorrected for the quartz prism dispersion or the lamp energy distribution, are shown in Fig. 8. The infrared response of PT 49 corresponds to the class III infrared response described in the previous report, while PT 47 and 48 correspond to class IV.

In the preparation of PT 47 and 48 the cesium addition was discontinued shortly after the second maximum in thermionic emission was passed. In PT 48 TE the oxygen content of the surface is 55% of that in PT 49 TE. Though these two cathodes differ appreciably in sensitivity they are similar in that the long wavelength limits exceed 1500 mμ, and the half maximum photocurrent wavelengths are 1075 and 1085 mμ for PT 47 and 48 respectively.

In the preparation of PT 49 the surface was oxidized to give a black oxide film containing  $3.5 \times 10^{-5}$  gram atom of oxygen. Simultaneously the cesium addition rate was increased from  $7.2 \times 10^{-8}$  to  $38.8 \times 10^{-8}$  moles

Fig. 8

Spectral Response Characteristics  
of cooled tubes.



per minute. This rate of addition corresponds to depositing 40.3 layers of cesium per minute, as compared to 7.5 layers per minute in PT 47 and 48.

After cooling and reheating PT 49 TS to 190°C as discussed in the previous section, the cesium source was warmed and cesium added until a conduction current appeared. The cesium source was then cooled. The conduction current gradually decreased and thermionic emission returned. The thermionic emission increased to 1050 ( $\text{mm} \times 10^{-5}$ ) range, whereas the earlier maximum was 1600 ( $\text{mm} \times 10^{-5}$ ) range. The infrared sensitivity lost during the addition of the excess cesium returned. Actually the response obtained with the various filters was comparable to that obtained during the first cooling of the cesium after passing the maximum thermionic emission. Cooling the tube to room temperature resulted in an increase in the sensitivity as observed earlier in the processing (Fig. 7C). The spectral response of the cathode after cooling to room temperature is typical of the commercial S-1 surfaces that have been examined in this laboratory. In the previous quarterly report this spectral response was designated as class III.

### C. PHOTOSURFACE COMPOSITION

As discussed in the previous report, the photosurface composition is to be investigated by using radioactive cesium and by x-ray diffraction methods. The radioactive cesium composition determination will provide data on the gross composition of the surface, while the x-ray diffraction investigation will provide a means for determining the principal constituents. During the past quarter the compositional study has been restricted to the development of the technique for preparing the radioactive photo-surface and determining the gross composition.



For the tracer experiments the tube design discussed in the previous report has been adopted as standard. The procedure for the fabrication of the tube has been modified to correspond to the procedure used in the preparation of PT 47, 48, and 49. With this procedure in which the thermionic and photoelectric emission are continuously determined, it should be possible to control readily the processing conditions.

Several experimental tubes have been prepared in which radioactive cesium was used. These cathodes, however, did not develop the desired infrared sensitivity. During their fabrication significant thermionic emission was not developed, and the cathodes did not possess the desired infrared response characteristics. The final compositions of these cathodes ranged from  $\text{Cs}_{0.75}\text{O}$  to  $\text{Cs}_{0.99}\text{O}$ . For the  $\text{Cs}_{0.75}$  tube the photoelectric response maximum was at 510 mμ, while the  $\text{Cs}_{0.99}\text{O}$  maximum was at 915 mμ.

The range of composition obtained in these cathodes is in part related to the technique previously used in the oxidation of the silver film. The cathodes are given a preliminary oxidation prior to outgassing, in order to roughen the silver surface. During this initial oxidation it has been difficult to initiate the oxidation in the glow discharge.

Consequently the oxidation was performed in the abnormal glow discharge region and some silver may have been sputtered on the tube walls. Sputtered silver which could be oxidized during the second glow discharge oxidation would result in an error in the determination of the amount of oxygen deposited on the cathode. The difficulty is being corrected by preliminary oxidation of the cathode in a separate vacuum system followed by decomposition of the oxide at 350°C. After the oxidation characteristics of the

cathode are determined, it is mounted in a tube envelope and a tube is fabricated using the procedure described in the first section of this report. By this means it has been possible to prepare silver film surfaces which appear to oxidize satisfactorily when mounted in an experimental tube. The cause of the initial resistance to oxidation is at present unknown. It is possible that absence of appreciable thermionic emission during the cesium addition to the tubes was related to the distribution of the oxide in the silver film.

#### D. THE CRYSTAL STRUCTURE OF CESIUM MONOXIDE

A previous report on the crystal structure of cesium monoxide based essentially upon x-ray powder data has indicated that the orange-yellow oxide of cesium crystallizes in the rhombohedral system in anti- $\text{CdCl}_2$  type layer structure ( $D_{3d}^5$ ), the observed parameter of cesium ions in the unit cell being  $u = 0.242$ , as compared with  $u = 0.25$  reported by Helms and Klemm. This gives:  $\text{Cs}^+ - \text{O}^{2-} = 3.01\text{\AA}$ , in good agreement with the value expected from the known ionic radii of  $\text{Cs}^+$  and  $\text{O}^{2-}$ ; and  $\text{Cs}^+ - \text{Cs}^+ = 3.77\text{\AA}$ , which is still considerably higher than  $2r_{\text{Cs}^+} = 3.36\text{\AA}$ . In this type of layer structure, one layer of  $\text{Cs}^+$  may be regarded as being sandwiched between another layer of  $\text{Cs}^+$  and a layer of  $\text{O}^{2-}$ , so the  $\text{Cs}^+$  ions are expected to be appreciably polarized; also, there will be considerable electrostatic repulsion between the two neighboring  $\text{Cs}^+$  layers; these two effects working in the same direction may account for the long  $\text{Cs}^+ - \text{Cs}^+$  distance.

In the present work, the single-crystal data for  $\text{Cs}_2\text{O}$  obtained previously have been carefully treated for absorption and temperature corrections, with the object of examining the polarization effect from the electron density map and determining the parameter more accurately.

A normal projection of electron density along the hexagonal a-axis and a line-section through the c-axis have been prepared. These give  $u = 0.243$ ,  $\text{Cs}^+ - \text{O}^{2-} = 3.00\text{\AA}$ , and  $\text{Cs}^+ - \text{Cs}^+ = 3.80\text{\AA}$ . The  $\text{Cs}^+$  appears to consist of an essentially spherical core of about 39 electrons and  $0.9\text{\AA}$  in radius, and a diffuse shell where the electron density contour is considerably affected by series termination errors in the Fourier synthesis. However, comparison of the line-sections from  $F_{\text{obs}} \cdot e^{-\frac{B_1 \sin^2 \theta}{\lambda^2}}$  and from  $F_{\text{calc.}} \cdot e^{-\frac{B_1 \sin^2 \theta}{\lambda^2}}$  consisting of the same number of terms indicates that the electron density in the diffuse shell of the  $\text{Cs}^+$  is relatively higher, by 3 - 4 electrons, on the side of the ionic center away from the  $\text{O}^{2-}$  layer than on the side near the  $\text{O}^{2-}$  layer; the diffuse shell also extends farther on the side away from the  $\text{O}^{2-}$  layer. Just how much of this is due to polarization and how much to experimental errors in the observed structure factors is not known.

The single crystal rotation spots exhibit the kind of layer-shearing disorder recently discussed by Brindley and Ogilvie (Acta Cryst. 5, 412, 1952) for the case of brucite,  $\text{Mg}(\text{OH})_2$ . From the vertical width of the 001-reflections on the a-axis rotation photograph ( $\text{CuK}\alpha$ ), the extent of shearing disorder in the  $\text{Cs}_2\text{O}$  crystal used appears to be quite small: only about a  $2^\circ$ -bend in the c-axis. This would result in lengthening the  $\text{Cs}^+ - \text{Cs}^+$  distance about  $0.06\text{\AA}$ . Consequently, much of this increase must be due to the polarization effect. A final report on this structure work is being prepared.

NOTE: In submitting this report it is understood that all provisions of the contract between The Foundation and the Cooperator and pertaining to publicity of subject matter will be rigidly observed.

Investigator Donald T. Cromer Date Nov. 3, 1952

Supervisor Edwin H. Lippert Date Nov 17, 1952

For The Ohio State University Research Foundation

Executive Director

*[Signature]*